IJE TRANSACTIONS A: Basics Vol. 35, No. 04, (April 2022) 657-674

International Journal of Engineering

Journal Homepage: www.ije.ir

Identification of Combined Power Quality Disturbances in the Presence of Distributed Generations using Variational Mode Decomposition and K-nearest Neighbors Classifier

M. Behzadi, M. Amirahmadi, M. Tolou Askari*, M. Babaeinik

Department of Electrical and Electronic Engineering, Semnan Branch, Islamic Azad University, Semnan, Iran

PAPER INFO

Paper history:
Received 27 October 2021
Received in revised form 19 December 2021
Accepted 23 December 2021

Keywords:
Power Quality
Distributed Generations
Identification
Variational Mode Decomposition
Wind Turbine
Photovoltaic

ABSTRACT

Identification of combined power quality disturbances in the modern power systems by considering the development of different types of loads and distribution generations has become increasingly important. The novelty of this paper comes from the accurate and fast identification of the combined power quality disturbances in the presence of different distributed generations and loads such as photovoltaic cell, wind turbine with doubly fed induction generators, diesel engines, electric arc furnace, DC machine, 6-pulse and 12-pulse rectifier loads. In this paper, the features are extracted using variational mode decomposition, just from voltage waveforms. To reduce the redundant data, dimension of features vector, and time, the Relief-F method and correlation feature selection method are applied on the extracted features and these two methods are compared together. In this paper, the K-nearest neighbors classifier is used to classify the multiple power quality disturbances. To verify the effectiveness of the proposed method, different scenarios such as misfiring, variation of sun radiation and wind speed, entrance and exit of loads, capacitors and distributed generators, different fault at the grid in half-load to full-load were simulated. This method can be used as an added algorithm for smart metering in modern and smart power systems.

doi: *10.5829/ije.2022.35.04a.05*

NOMENCLATURE

$A_k(t)$	Envolpe	$\overline{l_{ff}}$	Average feature-feature intercorrelation
α	Variance of noise	$M_j(c)$	Nearest misses in feature selection
C	Class	m	Repeat parameter in Relief-F
$class(\ )$	Class function	$P(C)$	Prior probability of class in Relief-F method
D_i	Sample of features	$\varphi_k(t)$	Phase
$diff(\ )$	Difference fumction	q	Number of components
F	Feature	R_s	Heuristic merit of a feature
$\hat{f}(\omega)$	Input signal	s	Counter of heuristic merit of feature
$G[F]$	Weight of feature	$value(\ )$	Value function
H_j	Nearest hits in feature selection	ω_k	Centeral frequency of modes in VMD
i, j, k	Mode number or counter	$\hat{\lambda}$	Lagrangian coefficient
$\overline{l_{cf}}$	Mean feature-class correlation	$u_k(t)$	Various modes of variational mode decomposition (VMD)

*Corresponding Author Institutional Email: m.askari@semnaniau.ac.ir (M. Tolo Askari)

Please cite this article as: M. Behzadi, M. Amirahmadi, M. Tolou Askari, M. Babaeinik, Identification of Combined Power Quality Disturbances in the Presence of Distributed Generations using Variational Mode Decomposition and K-nearest Neighbors Classifier, ***International Journal of Engineering, Transactions A: Basics*** Vol. 35, No. 04, (2022) 657-674

1. INTRODUCTION

Nowadays, power quality has become a very important issue in modern power systems [1]. The reason for the importance of power quality is its effects on electrical equipment. Electrical equipment is designed to work with sinusoidal waveforms. The existence of different types of power quality disturbances (PQDs) such as voltage sag or swell, interruption, transient, harmonics, notch, spike, flicker, etc. leads to failure and reduction of life of electrical equipment [2]. Also, some PQDs lead to incorrect energy measurement and mal-operation of the protection relay. Power quality disturbances occur individually or in the combination of events. In traditional networks, the sources of production of power quality events have been usually known for power quality experts. Entrance and exit of large loads, power plants, or capacitor banks are the sources of production of power quality in these systems. Furthermore, the existence of 6-pulse and 12- pulse rectifiers and occurring short-circuit faults in these systems lead to product PQDs. In modern power systems by increasing the penetration level of distributed generations (DGs) the different combinations of PQDs also have increased [3, 4]. The modern power systems have been contained of different DGs such as photovoltaic (PV) generator [5], wind turbine generator [6], gas turbine generator, diesel generator, and energy storage unit. Prasad et al. [7] haves introduced an approach to identify single as well as mixed PQDs in the power system connected to the grid in solar cells integrated DC micro-grid. The PQDs was analyzed by capturing the AC voltage signals from the PCC of the utility grid. Then, they proposed a developed combination morphological filter to increase the system robustness. A heuristic technique based on the deep learning method was proposed by Gonzalez-Abreu et al. [8]. This method has three stage from feature extraction of power networks and then carried out an adaptive pattern and finally using a neural network to detect disturbances. However, the DGs were neglected in this study. In addition, Shen et al. [9] have used a deep learning technique to monitor the power quality in electrical power systems by considering the DGs. Accordingly, signal processing based on VMD combined with deep learning to determine the times scales of multi-component signals and then to classify the disturbances, respectively. Furthermore, there are different loads such as electric arc furnaces (EAF), DC motors, and 6-pulse and 12-pulse rectifiers in these systems. Solar and wind energy have prominent characters of fluctuation, randomness, and intermittent. Entrance and exit of different DGs and fluctuation of their output power lead to different combined PQDs [6, 10]. Furthermore, inverter-based DGs such as PV generators generate different harmonic pollution. In a real modern power system, PQDs usually consists of a combination of the power disturbances and most power disturbances are non-stationary [2]. Therefore, recognizing the different combinations of PQDs is a necessity in the modern power system.

Most PQDs identification studies are divided into three stages: signal analysis, feature extraction, and pattern recognition [11]. For signal analysis, several methods have been proposed including Fourier transform (FT) [12], discrete Fourier transform (DFT) , short-time Fourier transform (STFT) [13], wavelet transform (WT) [14], discrete wavelet transform (DWT) [15], wavelet packet transform (WPT) [16], Hilbert transform, S-transform (ST) [17], multiple time-window spectrum estimation (MTW) [18]. These methods often have some inherent disadvantages. Fourier transform only extract frequency information from the waveforms. Some of these methods only extract time information from the waveforms. Time-frequency information about PQDs can be extracted through DFT and STFT, but in the transforms, the transient feature cannot be clearly expressed in a fixed window size. A combined method based on the Hilbert–Huang Transform (HHT) and long short-term memory (LSTM) was proposed by Rodriguez et al. [19]. Also, recurrent artificial neural network was implemented to detect PQDs. Although this approach has effective outcomes, the combined PQDs in the presence of DGs was neglected. Therefore, studies have shifted to WT and ST [20, 21]. But, the WT [22] alone cannot generate high quality features. In other words, its overall performance depends on the feature extraction and classification types. The accuracy of ST is low in detecting non-stationary transient disturbances. Furthermore, most of the mentioned methods have a high computational burden.

Another method of spectral decomposition that, unlike WT, does not require pre-selective functions is empirical mode decomposition (EMD). This algorithm was first introduced by Huang to decompose non-stationary signals which is based on the extremities of a signal and the extraction of its intrinsic mode functions (IMFs). Since this algorithm is based on the use of extremity points, it is not a reliable solution because these points are strongly influenced by noise and sampling. The correct performance of the EMD algorithm and its improved methods requires the use of a noiseless signal that is rarely in practical conditions. On the other hand, another disadvantage of EMD is the lack of strong mathematical principles that make it difficult to predict the behavior of the algorithm on different signals. Recently, a method for decomposition of non-stationary signals has been proposed which, unlike EMD, has a higher resistance to noise and sampling. This method, called variational mode decomposition (VMD), has been able to overcome the decomposition defects of non-stationary signals that were available in EMD.

In many studies, the massive use of VMD can be observed. But, it is rarely used in PQDs identification. Some of its applications have been implemented in literature [23, 24]. A wind speed interval forecasting model based on VMD and multi-objective problem was proposed by Wang and Cheng [23]. This model included forecasting and noise reduction beside combination module to provide precise wind speed forecast for power model operation. Based on the VMD, a two stage method for eliminating the noise of Magnetic resonance imaging (MRI) was proposed by Pankaj et al. [24]. The VMD was introduced by Pankaj et al. [24] as an efficient technique to sequestrate the image into its components or modes based on frequency. An approach was proposed by Jalilian and Samadinasab [25] for measuring and finding short term PQ events in power systems by using micro-phasor measurement units. This measurement devise was used to monitor the PQ phenomena. Furthermore, variational mode extraction method was used by Jalilian and Samadinasab [25] to identify and analyze the non-stationary signals.

Previous studies have typically used expert knowledge or engineering experience in the feature extraction stage [6]. These feature extraction methods use only the static features of the main waveform. On the other hand, in these methods, the feature selection is highly desirable. A feature extraction technique based on fractional Fourier transform (FRFT) and extreme learning machine (ELM) was proposed by Samanta et al. [26]. Although this technique was useful, it can be still improved by using the developed version of these methods in order to provide accurate model. Motlagh, and Foroud [27] have given a method to recognize PQDs based on adaptive chirp mode pursuit in order to extract the features. Also, the grasshopper algorithm was applied to optimize the parameters of suppurt vector machine (SVM) as the classifier.

This paper presents a novel PQDs identification method in the presence of different DGs and loads in a modern power system. To cope with the above mentioned problems, a high accuracy and high speed classification approach based on the VMD and k-nearest neighbors network (KNN) has been presented in this paper. In this paper, the VMD method is used to decompose the voltage signals. This method is a robust method to noise and sampling due to its strong relationship with Wiener filter. The results of different experiments on combined PQDs show that this method has better performance in extraction of PQD features than similar methods. Contrary to previous researches, different combination of PQDs and different scenarios of DGs and loads are considered in this paper. Often, in previous researches, mathematical equations have been used to create PQDs, but in this paper, real PQDs are created simultaneously in PSCAD software environment. The presence of different DGs such as PV, wind turbine with doubly fed induction generator (DFIG), diesel engine (DE) was investigated in this paper. Furthermore, different loads such as EAF, DC motors, and 6-pulse and 12-pulse rectifiers from half-load to full-load are investigated in this paper. In this paper, only the voltage signals are used to identify the combined PQDs. This issue will decrease the measurement equipment and increase the speed of the method. The novelties of this article can be briefed as follows:

1. This paper presents a new method for identifying combined PQDs based on VMD, Relief-F, and KNN in a modern power system.
2. This paper uses VMD as a noise-resistant decomposition method and its performance is compared with EMD.
3. Different combinations of PQDs in the presence of different loads and DGs such as EAF, DC motors, and 6-pulse and 12-pulse rectifiers, PV, wind turbine with DFIG, and DE from half-load to full-load have been considered in this paper.
4. In this paper, the variation of sun radiation and wind speed are considered in generating PQDs in modern power systems.

To evaluate the proposed method, different comparative results have been presented in this paper. Results of VMD have been compared with EMD method. The proposed method is evaluated by comparing the different distance functions of the neural networks and other feature selectors such as correlation based feature selection (CFS). The comprative results confirm that the proposed method has a high accuracy in identifying the combined PQDs.

2. PROBLEM DEFINITION

To clarify the problem, we define the problem in both traditional power systems and modern power systems.

2. 1. Power Quality Disturbances in the Traditional Power Systems In traditional power systems, the issue of power quality disturbances is related to the classic linear load, classic nonlinear loads, different faults occurrence, entrance and exit of large loads, power plants, or capacitor banks [28]. Impulse transient PQDs are usually produced by switching loads, capacitor banks, or reactors in the traditional power systems. Voltage sag events are often produced by starting heavy engine loads or other heavy loads in the traditional power systems. Voltage swell event is often produced by single-phase faults. Under or over voltage events are often caused by load changes. Non-uniform distribution of single-phase loads or different transmission line specifications caused unbalanced voltage event in the traditional power systems. Harmonics are generated by nonlinear load such as EAF, DC motors, 6-pulse, and 12-pulse rectifiers, etc. in the traditional power systems. Flicker events are often produced by starting heavy engine loads in the traditional power systems [29]. By increasing the penetration level of DGs, identification of PQDs has become more complex and traditional power systems have changed to the modern power systems.

2. 2. Power Quality Disturbances in the Modern Power Systems In a modern power system, different DGs with different operations are added to the traditional power system. Adding different DGs leads to generate different combined PQDs in the modern power systems [28]. Identification of different combined PQDs is a big challenge in the modern power systems. In these systems, entrance and exit of different DGs lead to generate voltage swell and sag events, respectively [6, 10]. On the other hand, environmental changes such as variation in solar insolation and change in wind greatly change voltage profile in these systems [30, 31]. Furthermore, increasing penetration level of DGs with inverter such as wind turbine and PV lead to increase harmonics in the modern power system [32]. In the modern power systems, some events in diesel-engine driven generators such as misfiring in cylinders, and gearbox tooth crashing lead to generate flicker [33]. Also, some events in wind turbines such as tower shadow, wind shear, turbine blade break down, and blade pitching errors lead to generate flicker in the modern power systems [34]. To identify different combined PQDs in the modern power systems, a new method is presented in this paper.

3. PROPOSED ALGORITHM

The proposed method generally has the following four main steps (Figure 1):

1. Data generation using different loads and DGs simulations in PSCAD/EMTDC simulation program (version 4.5) in different scenarios.
2. Feature extraction using VMD.
3. Feature selection using Relief-F.
4. Classification of PQDs using KNN.

3. 1. Data Generation Using PSCAD Data generation is an important challenge in the issue of identification of PQDs. These data must be close to the real data in the power system. Therefore, in this step, PQDs are really generated in different scenarios in PSCAD software environment such as connecting different linear, non-linear loads, capacitive banks, and DGs. Different loads are simulated in PSCAD, including EAF, DC motors, and 6-pulse and 12-pulse rectifiers. Different DGs are simulated, including PV, wind turbine with DFIG, and DE. Loads are altered from half-load to full-loads. Also, the rate of active and reactive power of DGs is altered from half-load to full-load.

3. 2. Feature Extraction using VMD Another challenge in the issue of identification of PQDs is a complete feature extraction. This feature extraction must be extract time and frequency information together. VMD is a time-frequency decomposition approach for robust analyzing adaptive, stationary and non-stationary signals [35]. Variational mode decomposition uses a new definition of IMFs and, unlike EMD, which considers IMFs as signal oscillating components, introduces them as amplitude-frequency modulation (AM-FM) signals in Equation (1) [36]:

$$u_k(\mathrm{t}) = \mathrm{A}_k(t)\cos(\varphi_k(t)) \tag{1}$$

where k is the mode number, $\varphi_k(t)$ is the phase, $\mathrm{A}_k(t)$ is the envelope and non-negative ($\mathrm{A}_k(t) \geq 0$). It is notable that, envelope $\mathrm{A}_k(t)$ and instantaneous

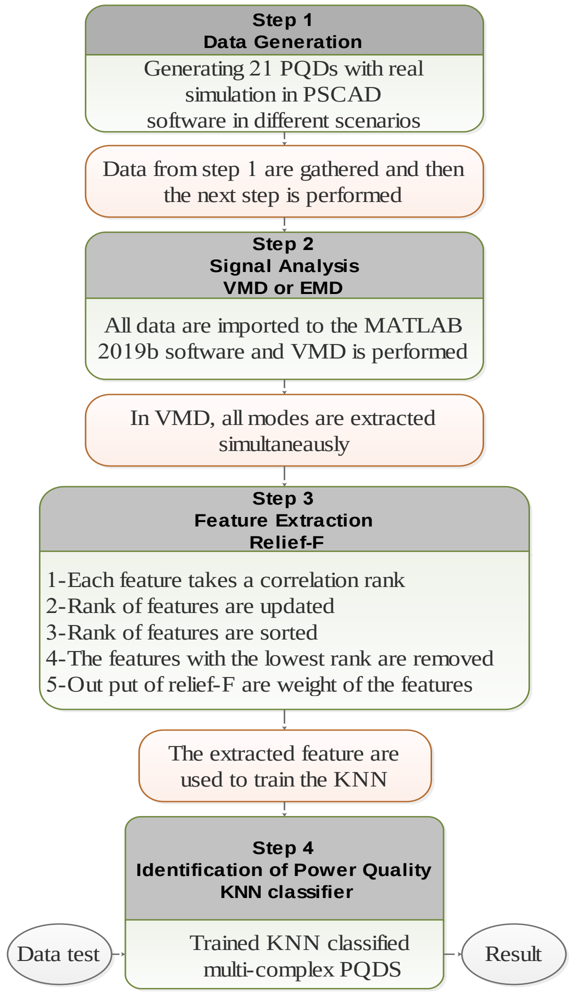

Figure 1. Flowchart of the methodology

frequency (equal to the phase derivative i.e. $\omega_k(t) = \varphi_k'(t)$) much slower than phase $\varphi_k(t)$ changes. Therefore, $u_k(t)$ mode can be introduced as a pure harmonic of signal with amplitude $A_k(t)$ and instantaneous frequency $\varphi_k'(t)$ in a suitable time frame. This new definition of the IMF leads to the creation of a narrow band signal, which is the main assumption of this method in the separation of modes.

In this method, each IMF is a finite band signal around a central frequency, which the value of the central frequency is estimated at any given moment as real-time. In fact, due to the strong relationship between VMD and Wiener filter, this method is more resistant to noise. In VMD, all modes are extracted simultaneously, while this is done in EMD through recursive operations. Variational mode decomposition includes Weiner filter for noise, Hilbert transform to reconstruct signal side-band, and shift the signal frequency by multiplying a mixed exponential function [35]. All modes in the frequency domain are directly updated. By using the Hermitian symmetry, the frequency spectrum of different mode signals is easily obtained. The real component of the reverse Fourier transformation of this filtered signal transmits the mode to the time domain. In this method, k mode in the frequency domain in the n replication can be computed by the Equation (2) [35]:

$$\hat{u}_k^{n+1}(\omega) = \frac{\hat{f}(\omega) - \left(\sum_{i<k}\hat{u}_i(\omega) + \sum_{i>k}\hat{u}_i(\omega) - \frac{\hat{\lambda}(\omega)}{2}\right)}{1 + 2\alpha(\omega - \omega_k)^2} \tag{2}$$

where $\hat{f}(\omega)$ is the input signal in the frequency domain, α is the variance of noise and $\hat{\lambda}$ is the Lagrange coefficient for minimization. This equation is exactly like filtering current residual by Wiener filter. The central frequency of each mode is updated as Equation (3) [35]:

$$\omega_k^{n+1} = \frac{\int_0^\infty \omega |\hat{u}_k(\omega)|^2 \, d\omega}{\int_0^\infty |\hat{u}_k(\omega)|^2 \, d\omega} \tag{3}$$

The center of gravity of the power spectrum modes is this new ω_k. By repeating the above process in case of convergence, the decomposed modes are calculated.

Variational mode decomposition provides different modes to extract features. In this paper, to decrease the features, time, and the redundant data, Relief-F and CFS methods is applied as a filter tool.

3. 3. Feature Selection using Relief-F and CFS Appropriate feature selection among a large number of features is an important challenge in classification problems. The reasons of feature selection are the reduction of the redundant data, number of features and, time. In this paper, we use Relief-F and CFS methods as two tools for feature selection. Furthermore, in this paper, these two methods are compared together.

3. 3. 1. Relief-F Relief-F is a feature selection algorithm that is used to reduce the size of the problem. The Relief-F method is a robustness method and appropriate method for multiclass problems. The steps of the Relief algorithm, as an algorithm to reduce the dimensions of input data, are as follows: in the first step, each feature takes a correlation rank based on their relationship with the final goal. In the second step, the ranks are updated using randomly selected samples. Then these ranks are sorted and features with the lowest rank are removed, (a threshold is used for features ranking). The remaining features are saved as superior features and are introduced as inputs of a classifier algorithm. In other words, in Relief-F method, each feature initially takes a weight, and then the weight is updated by using the value of the feature for each sample. The outputs of Relief-F method are the values of the weight of features. The output of Relief-F method is calculated as Equation (4) which contains several loops [37]:

$$G[F] = G[F] - \sum_{j=1}^{k} \frac{diff(F, D_i, H_j)}{m.k} + \sum_{C \neq class(D_i)} \left[\frac{\frac{P(c)}{1 - P(class(D_i))} \sum_{j=1}^{k} diff(F, D_i, M_j(C))}{m.k} \right] \tag{4}$$

The used parameters have been introduced in nomenclature. The difference between the values of the feature F for two samples D and H is computed by function $diff(F, D, H)$ as expressed by Equations (5) and (6) [37]:

- if one sample has been determined:

$$diff(F, D, H) = 1 - P(value(F, H) | class(D)) \tag{5}$$

- if both samples have not been determined:

$$diff(F, D, H) = 1 - \sum_{V}^{values(F)} (P(V \mid class(D)) \times P(V \mid class(H))) \tag{1}$$

3. 3. 2. Correlation Feature Selection (CFS) Feature selection based on correlation is a powerful method for filtering that ranks feature subsets according to a correlation based heuristic evaluation function. The correlation method points to subsets that have properties with the highest correlation coefficient with the desired sample class [37]. Subsets that have the most points are considered as the main variable. The objective is to decrease feature-to-feature correlation and increase feature-to-class correlation. The evaluation function of the CFS algorithm is presented in Equation (7) [37]:

$$R_s = \frac{q\overline{I_{cf}}}{\sqrt{q + q\,(q-1)\overline{I_{ff}}}} \tag{7}$$

The used parameters have been introduced in nomenclature. The algorithm has a high ability to quickly detect unrelated and additional data.

3. 4. Identification of Combined PQDs using KNN

In this section, the extracted and selected features are used to train the classifier. In these years researchers are eager to use KNN as a power quality disturbance classifier because of high speed and accuracy, less-parametric, user- friendly frame, being compatible with oscillatory trends of electrical measurements.

K-nearest neighbors performs classification based on the data similarity. In fact, for each new test data, it calculates the near neighbor k distances and tags a ticket similar to the train data. In other words, in the KNN classifier, an unknown sample (test data) is classified based on the similarity with a known sample (train data) based on calculating the distance between them. For this reason, the KNN classification algorithm is dependent on the selected distance function. In the previous researches, different distance functions such as Cosine distance, Correlation distance, Cityblock distance, Euclidian distance have been used [38]. Selecting the appropriate distance function for the data set is an important issue. In this paper, the performance of four distance functions for PQDs data is compared together and the appropriate distance function is introduced. Each distance functions has advantages and disadvantages, for example, in Euclidean distance, the data amplitude has a great impact on the accuracy of classification. In the Cityblock distance, the computing volume is lower and the speed is higher. In the Cosine distance, the amplitude difference between the samples is not known. In this paper, KNN performance is investigated using different distance functions on the combined PQDs. Other hands, it is compared with PNN [39] network to introduce the best distance function.

4. SIMULATION AND RESULTS ANALYSIS

To verify the proposed method, different types of loads and DGs have been simulated in PSCAD/EMTDC simulation program (Version 4.5). Table 1 presents the sources of PQDs and grid conditions.

Figure 2 shows the simulated network. This network consists of four nonlinear loads, three DGs, one set capacitive bank, and one linear load. Nonlinear loads include EAF, DC motors, and 6-pulse and 12-pulse rectifiers. Distributed generations include PV, wind turbine, and DE.

Table 2 presents 21 classes of PQDs that were considered in this paper. Class 1 was dedicated to flicker sources. Wind turbine (aerodynamic), electric arc furnace, and diesel engine were considered as flicker sources. Classes 2 to 5 were dedicated to double combinations of flicker and other PQDs. For example, in the presence of wind turbine, EAF or DE, switch on or switch off a large load are lead to Flicker+Sag or Flicker+swell PQDs. Other scenarios in the presence of wind turbine, EAF, or DE are double line to ground (LLG) fault or switching a large capacitor that leads to Flicker+Interrupt or Flicker+Impulse PQDs. Class 6 was dedicated to harmonic sources include: wind turbine (power electronic), PV, 6-pulse, 12-pulse, and DC machine. Classes 7 to 10 were dedicated to double combinations of harmonic and other PQDs. For example, in the presence of wind turbine, PV, 6-pulse, 12-pulse, or DC machine switch on or switch off a large load are lead to Harmonic+Sag or Harmonic+Swell PQDs. Other scenarios such as LLG fault and switching a large capacitor are added to the mentioned harmonic sources. It is notable that wind turbines alone can be the cause of generating flicker and harmonic [34, 40]. Combined PQDs were introduced in classes 11 to 15. Finally, single PQDs were introduced in classes 16 to 21.

To generate data, different scenarios are implemented in this network (Table 2). Different scenarios such as misfiring, variation of sun radiation and wind speed, entrance and exit of loads, capacitors and DGs, different fault at the grid in half-load to full-load.

The capacity of PV is considered 1.6 MW which is modelled using 10 equal units in parallel mode. The output converter is 500 V DC. This DC voltage is converted into 480 V 3-phase AC power with an inverter. The variations in solar insulation are simulated in the variation of output power from half capacity to full capacity.

The capacity of wind turbine is considered 1.5 MW which is modelled as DFIG in 3-phase. The rated of wind speed is considered equal to 14 m/s.

TABLE 1. Details of simulated network

#	Load or DGs	Element	Conditions
1	6 pulse rectifier	PCC Voltage	20 kV
2	12 pulse rectifier		
3	DC machine (DM)	Z Line	0.007+0.004231j
4	EAF		
5	Photovoltaic (PV)	Z Grid	2.5+15j
6	Wind turbine		
7	Diesel engine (DE)	Grid Voltage	20kV
8	Capacitor bank	Short Circuit Power	20MVA

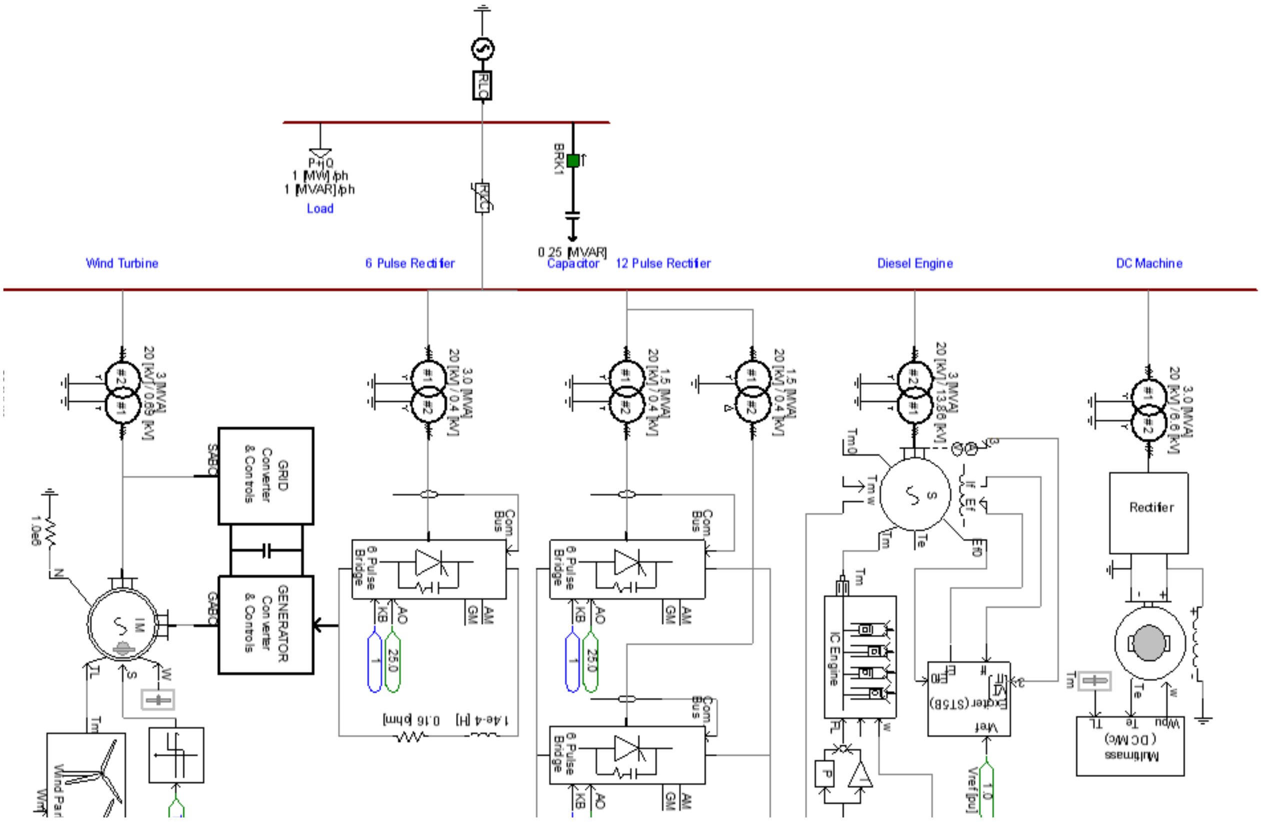

Figure 2. Schematic of the simulated network in PSCAD software

TABLE 2. Classes of combined power quality disturbances and their sources

Class	PQDs	Sources				
PQ1	Flicker	Wind turbine (aerodynamic)	EAF (coherence of Load)		DE (misfiring)	
PQ2	Flicker+Sag	Switch On a Large Load	Switch On a Large Load		Switch On a Large Load	
PQ3	Flicker+Swell	Switch Off a Large Load	Switch Off a Large Load		Switch Off a Large Load	
PQ4	Flicker+Interrupt	LLG	LLG		LLG	
PQ5	Flicker+Impulse	Switching a Large Capacitor	Switching a Large Capacitor		Switching a Large Capacitor	
PQ6	Harmonic	Wind turbine (power electronic)	PV	6 pulse rectifier	12 pulse rectifier	DC machine
PQ7	Harmonic+Sag	Switch On a Large Load	Switch On a Large Load	Switch On a Large Load	Switch On a Large Load	Switch On a Large Load
PQ8	Harmonic+Swell	Switch Off a Large Load	Switch Off a Large Load	Switch Off a Large Load	Switch Off a Large Load	Switch Off a Large Load
PQ9	Harmonic+Interrupt	LLG	LLG	LLG	LLG	LLG
PQ10	Harmonic+Impulse	Switching a Large Capacitor	Switching a Large Capacitor	Switching a Large Capacitor	Switching a Large Capacitor	Switching a Large Capacitor
PQ11	Harmonic+Flicker	Wind turbine (power electronic + aerodynamic)				
PQ12	Harmonic+Flicker+ Sag	Switch On a Large Load				
PQ13	Harmonic+Flicker+ Swell	Switch Off a Large Load				

PQ14	Harmonic+Flicker+Interrupt	LLG
PQ15	Harmonic+Flicker+Impulse	Switching a Large Capacitor
PQ16	Normal	Normal Linear Load
PQ17	Sag	Switch On a Large Load
PQ18	Swell	Switch Off a Large Load
PQ19	Interrupt	LLG
PQ20	Impulse	Switching a Large Capacitor
PQ21	Notch	Normal Linear Load+Capacitor

100 samples for train and 100 samples for the test are considered for any classes. The proposed methods were developed under the MATLAB environment version 9.7 on a Windows 10 with an Intel CORE i7 Pro processor and 12-GB RAM.

According to subsection 3.1, the first stage is data generation using accurate simulation in PSCAD software. All scenarios in Table 2 were implemented to generate the different combinations of power quality events. A complete database from different voltage waveforms was generated in different scenarios in PSCAD software. Some of the voltage waveforms of PQDs with their modes are shown in Figure 3. According to subsection 3.2, main voltages were decomposed to 10 modes using VMD. In Figure 3, the vertical and horizontal axes show the voltage amplitude and time, respectively. The voltage amplitude was normalized to the PCC voltage

To have powerful features, mathematical features such as mean value, the area under, kurtosis, second moment, third moment, fourth moment, skewness, and standard deviation (STD) were extracted from obtained modes (Table 3). The first ten features are assigned to the mean value of modes 1-10. The second ten features are assined to the area under the modes 1-10. The third ten features are assigned to the kurtosis of modes of 1-10. The fourth ten features are assigned to the second moment of modes of 1-10. The fifth ten features are assigned to the third moment of modes of 1-10. The sixth ten features are assigned to the forth moment of modes of 1-10. The seventh ten features are assigned to the skewness of modes of 1-10. The eighth ten features are assigned to the STD of modes of 1-10. In the next stage, these 80 extracted features are filtered. The reason and method of filtering were described in subsection 3.3. The results of filtering by Relief-F method are presented in Table 4. The features with greater discriminating power located in the higher rank. In Table 4, features 24, 26 and 29 are the three features with the highest rank, . Features 33, 80 and 52 also have the lowest rank among the selected features. In other words, features 24, 26, and 29 have the most weight to separate PQD signals. Features 33, 80 and 52 also have the least weight in separating PQDs signals.

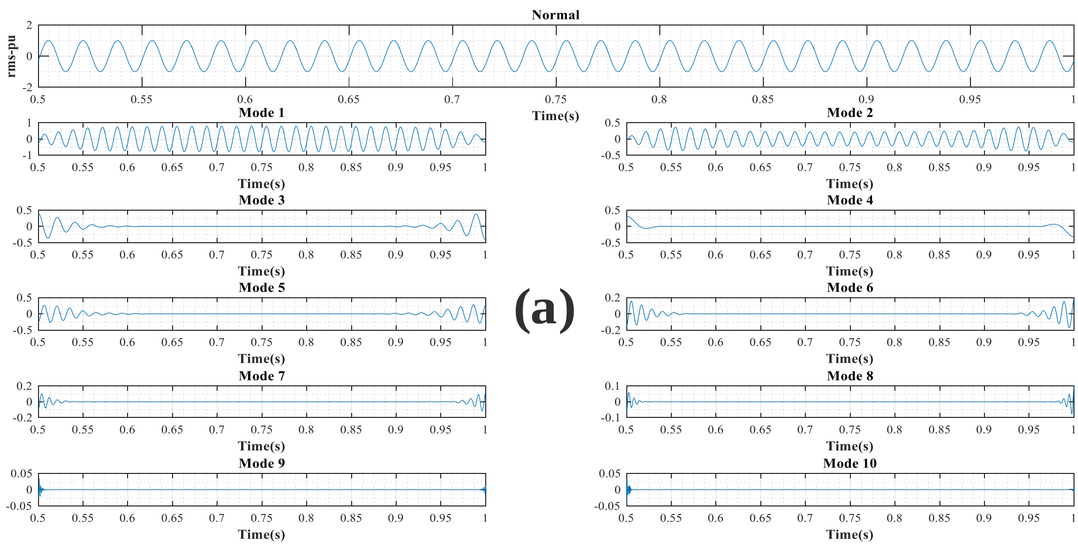

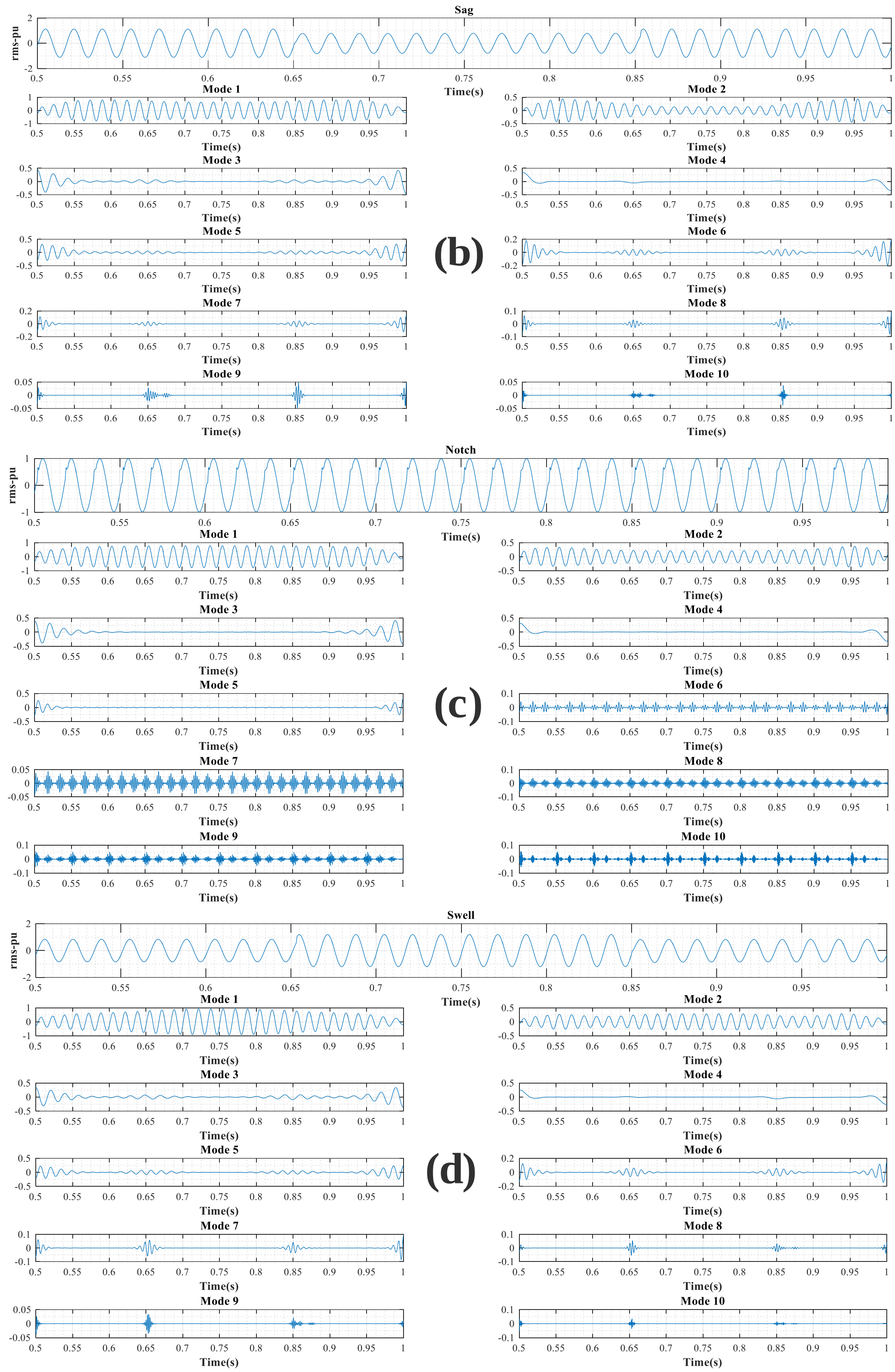
Sag
rms-pu
Time(s)
Mode 1
Mode 2
Mode 3
Mode 4
Mode 5
Mode 6
Mode 7
Mode 8
Mode 9
Mode 10
(b)
Notch
rms-pu
Time(s)
Mode 1
Mode 2
Mode 3
Mode 4
Mode 5
Mode 6
Mode 7
Mode 8
Mode 9
Mode 10
(c)
Swell
rms-pu
Time(s)
Mode 1
Mode 2
Mode 3
Mode 4
Mode 5
Mode 6
Mode 7
Mode 8
Mode 9
Mode 10
(d)

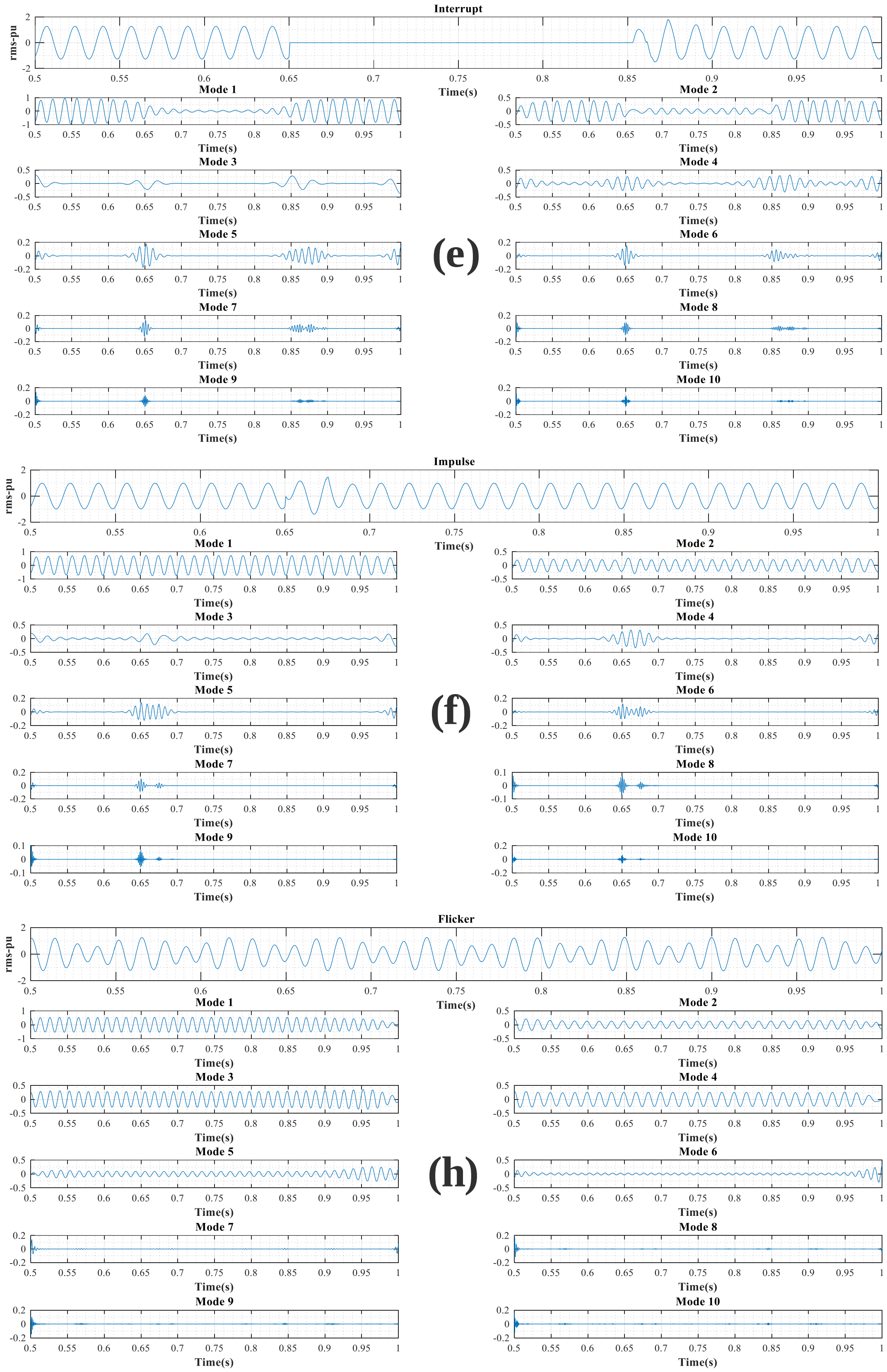

Figure 3. Power quality disturbances with their extracted modes using VMD: (a) normal; (b) sag; (c) notch; (d) swell; (e) interrupt; (f) impulse; (g) harmonic; (h) flicker

TABLE 3. Extracted features from VMD

Number	Feature
1-10	Mean value of modes 1-10
11-20	Area under the modes 1-10
21-30	Kurtosis of modes of 1-10
31-40	Second moment of modes of 1-10
41-50	Third moment of modes of 1-10
51-60	Forth moment of modes of 1-10
61-70	Skewness of modes of 1-10
71-80	STD of modes of 1-10

Table 5 provides a comparison between neural networks, distance functions, and feature selectors. Furthermore, the impact of features dimensions summarized in Table 5. Even in the PNN classifier, the relief-F feature selector performance is better than the CFS. Using relief-F and PNN the time and accuracy of classification were obtained 2.09 seconds and 96.80%, respectively, whereas using CFS and PNN the time and accuracy of classification were obtained 2.356 seconds and 96.00%. The result show that the performance of relief-F is better than CFS in this problem. In other hand, the performance of the KNN classifier is better than the PNN classifier in all distance functions. The highest classification accuracy was obtained using KNN classifier with Cityblock distance function (99.74%). The performance of Relief-F and CFS methods were compared in Table 6. The results show that the performance of the Relief-F method is better than the CFS method in this problem.

To the best of the authors' knowledge, the different combinations of three PQDs in the presence of DGs have rarely been presented in previous studies. In this paper, different and complex combinations of PQ events have been considered in 21 classes. The performance of the Cityblock distance function of KNN is better in terms of accuracy and consumed time. Details of accuracy in each class and total accuracy are presented in Table 6. The lowest classification accuracy is 99.02% in the identification of combination of Harmonic+Flicker+Interrupt. The highest accuracy of classification with 100% belongs to individual class, such as sag, swell, interrupt, and etc. It is notable that total accuracy is 99.74%.

TABLE 4. Rank of features using Relief-F

Rank	Feature	Weight	Rank	Feature	Weight	Rank	Feature	Weight	Rank	Feature	Weight
1	24	0.044817	21	16	0.010226	41	41	0.001009	61	5	0.001007
2	26	0.040434	22	65	0.009717	42	10	0.001008	62	42	0.001005
3	29	0.039383	23	64	0.009466	43	9	0.001008	63	4	0.001004
4	30	0.033054	24	17	0.007994	44	7	0.001008	64	36	0.001003
5	69	0.030889	25	18	0.007615	45	49	0.001008	65	37	0.001003
6	28	0.027448	26	22	0.006496	46	8	0.001008	66	39	0.001003
7	25	0.026843	27	20	0.005340	47	47	0.001008	67	2	0.001003
8	67	0.024697	28	19	0.004910	48	46	0.001008	68	40	0.001002
9	27	0.024424	29	63	0.004186	49	48	0.001008	69	38	0.001001
10	11	0.023712	30	71	0.003423	50	59	0.001008	70	76	0.000999
11	66	0.021257	31	62	0.003188	51	57	0.001008	71	3	0.000998
12	68	0.020584	32	1	0.002554	52	50	0.001008	72	53	0.000997
13	23	0.020296	33	31	0.002152	53	45	0.001008	73	35	0.000995
14	13	0.018209	34	72	0.001613	54	56	0.001008	74	32	0.000988
15	15	0.013704	35	73	0.001482	55	60	0.001008	75	77	0.000952
16	70	0.013252	36	51	0.001460	56	58	0.001008	76	78	0.000945
17	14	0.012604	37	74	0.001378	57	6	0.001008	77	79	0.000939
18	61	0.012226	38	75	0.001129	58	55	0.001008	78	33	0.000934
19	12	0.010971	39	34	0.001038	59	44	0.001008	79	80	0.000931
20	21	0.010867	40	54	0.001012	60	43	0.001007	80	52	0.000919

TABLE 5. Comparative results between classifiers, feature selectors, and feature dimensions

Classifier	distance function	Feature selector	Sets of features	Time assumed(s)	Classifier accuracy (%)
PNN	Gaussians	Relief-F	First 19 Features	2.085081	96.80
		CFS	First 22 Features	2.359369	96.00
KNN	Cityblock	Relief-F	First 20 Features	**0.268652**	**99.74**
		CFS	First 21 Features	0.275225	99.39
	Correlation	Relief-F	First 21 Features	0.280029	98.93
		CFS	First 21 Features	0.299565	98.46
	Euclidian	Relief-F	First 20 Features	0.319245	98.76
		CFS	First 20 Features	0.345749	98.46
	Cosine	Relief-F	First 19 Features	0.312949	98.83
		CFS	First 22 Features	0.3144207	98.46

TABLE 6. Performance of the KNN-Cityblock classifier

Class	Accuracy	Class	Accuracy	Class	Accuracy	Class	Accuracy
Normal	100 %	Harmonic	100 %	Flicker	100 %	Harmonic+Flicker	99.74 %
Sag	100 %	Harmonic+Sag	99.87 %	Flicker+Sag	99.83 %	Harmonic+Flicker+Sag	99.16 %
Swell	100 %	Harmonic+Swell	99.76 %	Flicker+Swell	99.85 %	Harmonic+Flicker+Swell	99.05 %
Interrupt	100 %	Harmonic+Interrupt	99.75 %	Flicker+Interrupt	99.72 %	Harmonic+Flicker+Interrupt	99.02 %
Impulse	100 %	Harmonic+Impulse	99.85 %	Flicker+Transient	99.82 %	Harmonic+Flicker+Impulse	99.12 %
Notch	100 %						
Total Accuracy				**99.74 %**			

To validate the proposed method, some 3D figures of separation results are shown in Figure 4. In these figures, different PQ events were compared together. The first figure shows the individual PQ events. Other figures show different combinations of PQ events. The results show that the proposed method identifies the combined PQDs with high accuracy and speed in the presence of different types of DGs.

To investigate the performance of the proposed method in noisy conditions, a new scenario have been added to this paper. Three SNR levels of Gaussian noise include 20 dB, 30 dB, and 50 dB have been considered. Table 7 shows the comparative results between EMD and VMD in noisy conditions. Variational mode decomposition, unlike EMD, is robust against noise. The proposed method classifies the PQDs and their sources simultaneously with high accuracy even in noisy conditions.

In Table 8 the assumptions and results of this paper have been compared with other papers in this issue. Unlike other papers, this paper has the highest number of classes. Twenty- one multi-complex PQDs have been

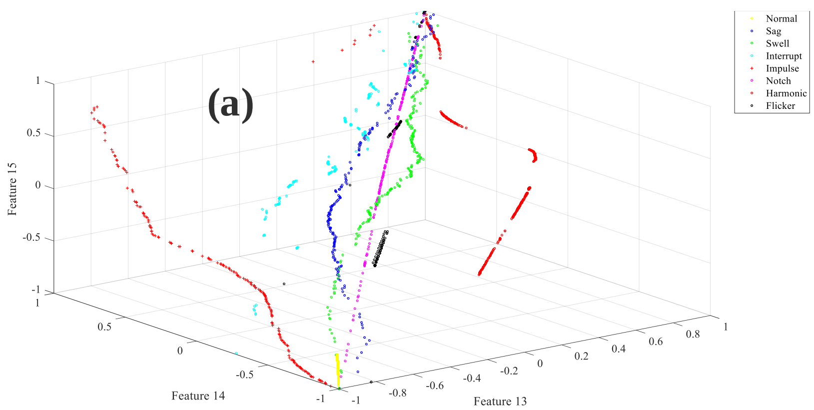

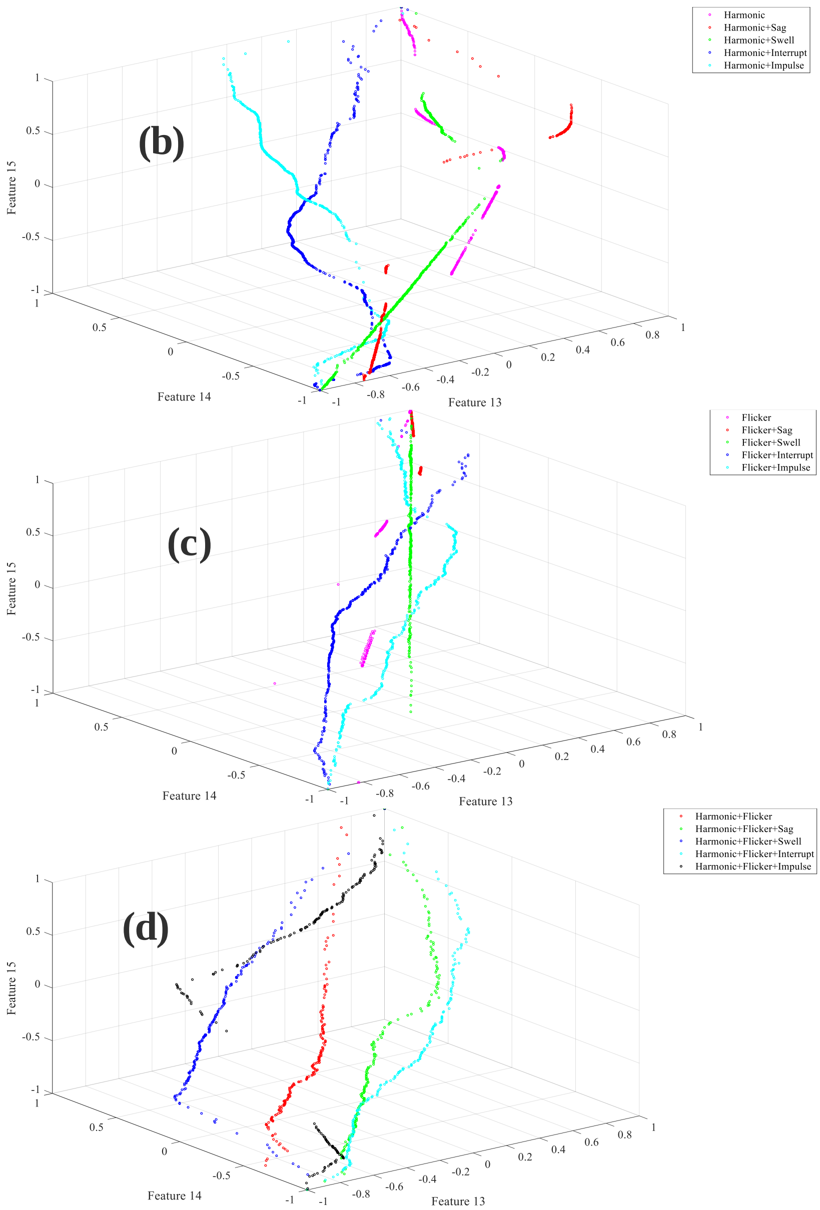

Figure 4. 3D figures of separation results: (a) individual PQDs; (b) double combination of harmonic disturbances; (c) double combination of flicker disturbances; (d) triple combination of PQDs

TABLE 7. Comparative results between EMD and VMD in noisy conditions

	Accuracy							
	PQDs classification				**Source identification**			
	Noiseless	**20 dB**	**30 dB**	**50 dB**	**Noiseless**	**20 dB**	**30 dB**	**50 dB**
EMD-KNN	97.65	91.55	93.22	96.57	98.48	95.63	96.87	98.15
VMD-KNN	99.74	99.05	99.21	99.34	99.87	99.58	99.69	99.79

considered in this paper. For this reason, it is not fair to compare the accuracy of classification regardless of the number of classes. However, the accuracy of the classification of the proposed method in this paper is very desirable in noiseless and noisy mode. The listed papers have not considered the issue of penetration of DGs in

HMP systems [15, 20, 21, 41-45]. But in this paper, three types of DGs including wind turbine, PV, and DE have been considered. Shen et al. [10], Saini and Beniwal [31] only considered wind turbine as DGs. Contrary to other papers, we have considered different scenarios such as misfiring, variation of sun radiation and wind speed, entrance and exit of loads, capacitors and distributed generators, different faults at the grid in half-load to full-load in this paper. The listed papers in Table 8 have not addressed the issue of identifying the source type of PQDs, whereas in our paper, in addition to categorizing the multi-complex PQDs, the source type of PQDs is simultaneously identified. We believe the proposed approach can be used as an added algorithm for smart metering in modern and smart power systems.

For the purpose of verifying method, mentioned loads and DGs have connected to 34 bus radial distribution system in PSCAD. Table 9 presents the sources of PQDs and grid conditions [46]. Figure 5 shows the simulated network. This network consists of four nonlinear loads, three DGs, one set capacitive bank, and one linear load. Nonlinear loads include EAF, DC motors, and 6-pulse and 12-pulse rectifiers. Distributed generations include PV, wind turbine, and DE.

For second test system, details of accuracy in each class and total accuracy are presented in Table 10. The lowest classification accuracy is 98% in the identification of combination of Harmonic+Interrupt AND Harmonic+Flicker+Impulse. The highest accuracy of classification with 100% belongs to individual classes, such as normal load, impulse, notch, and etc. It is notable that total accuracy is 99.55%.

The future direction of this research is to use this method in smart meters as an additional tool. So that new power quality meters can be produced with the ability to identify and classify power quality events. On the other hand, this proposed method can be added to existing power quality meters as a tool. It is noteworthy that the proposed method can be added in PMUs in transmission networks and in micro PMUs in distribution networks and lead to accurate identification and classification of power quality events. The limitations of this proposed method are related to its technology and industrialization. On the other hand, all power quality event classes must be trained to the classifier.

TABLE 8. Comparison of this paper with other papers

Method	Sources identification	# classes	# Features	# DGs types	accuracy			
					normal	20 dB	30 dB	50 dB
IPCA+ 1-D-CNN [10]	No	12	72	1	99.92	99.76	-	99.85
WT+ST [15]	No	8	20	0	99.81	97.69	99.31	-
DWT+HST [43]	No	9	26	0	99.77	99.22	99.77	-
DWT+PNN [44]	No	16	9	0	99.875	93.6	95.5	-
ST [42]	No	14	5	0	99.43	97.96	99.29	-
OMFST + CA [21]	No	12	67	0	-	91.50	98.58	98.92
VMD+SVM [47]	No	17	3	1	99.03	-	-	-
VMD+ELM [45]	No	14	4	0	99.71	99.3	99.7	-
WT+LSSVM [20]	No	4	21	0	99.71	-	-	-
NSGA III+DAG-SVM [41]	No	8	2	0	99.85	99.15	99.35	-
FTT+SR-ELM [31]	No	12	107	1	99.59	-	95.29	97.93
This paper	**Yes**	**21**	**20**	**3**	**99.74**	**99.05**	**99.21**	**99.34**

TABLE 9. Details of simulated network

Element	Conditions
PCC Voltage	24.9 kV
Z Grid	0.16038+j0.64151ohm
Grid Voltage	24.9kV
Short Circuit Power	12MVA

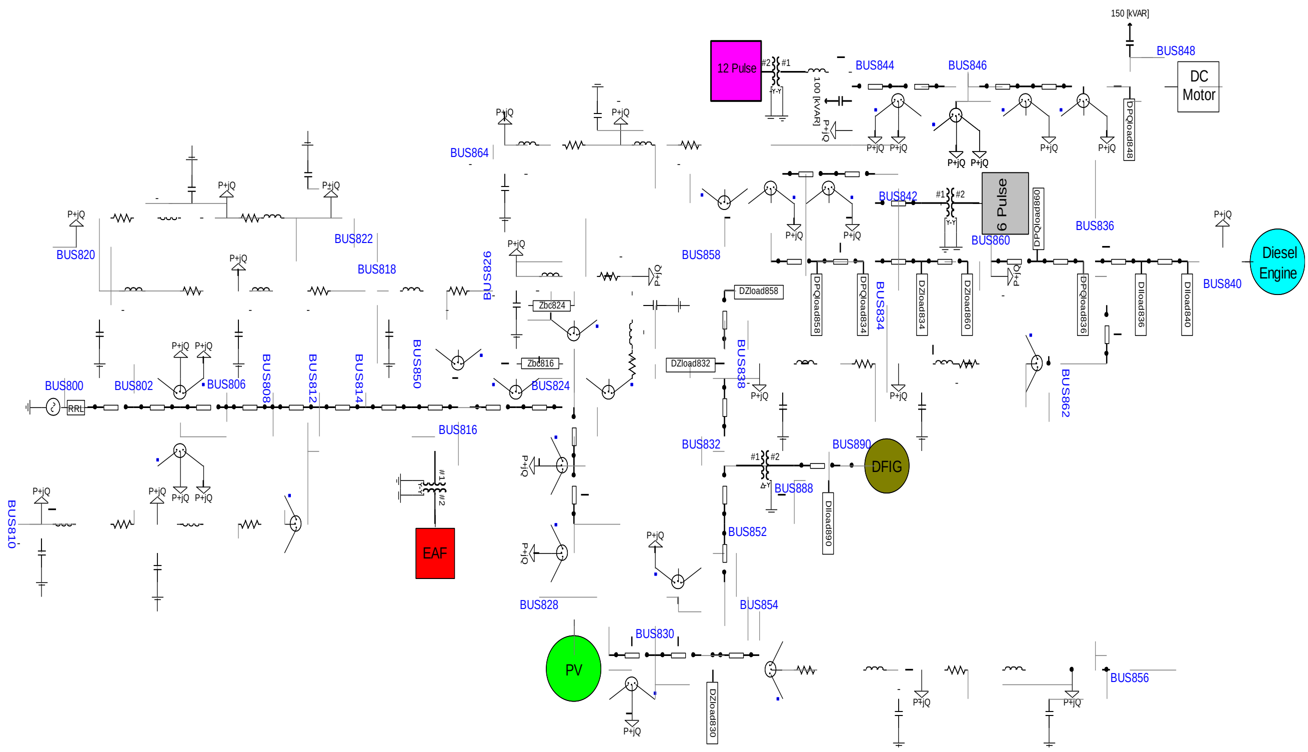

Figure 4. Schematic of 34 bus distribution grid [46]

TABLE 10. Performance of the KNN-Cityblock classifier in second test system

Class	Accuracy	Class	Accuracy	Class	Accuracy	Class	Accuracy
Normal	100	Harmonic	99.95	Flicker	99.76	Harmonic+Flicker	99.00
Sag	99.95	Harmonic+Sag	99.64	Flicker+Sag	99.94	Harmonic+Flicker+Sag	99.15
Swell	99.81	Harmonic+Swell	99.65	Flicker+Swell	99.50	Harmonic+Flicker+Swell	99.36
Interrupt	99.96	Harmonic+Interrupt	98.00	Flicker+Interrupt	99.48	Harmonic+Flicker+Interrupt	99.68
Impulse	100.00	Harmonic+Impulse	99.91	Flicker+Transient	99.86	Harmonic+Flicker+Impulse	98.00
Notch	100.00						
Total Accuracy				**99.55%**			

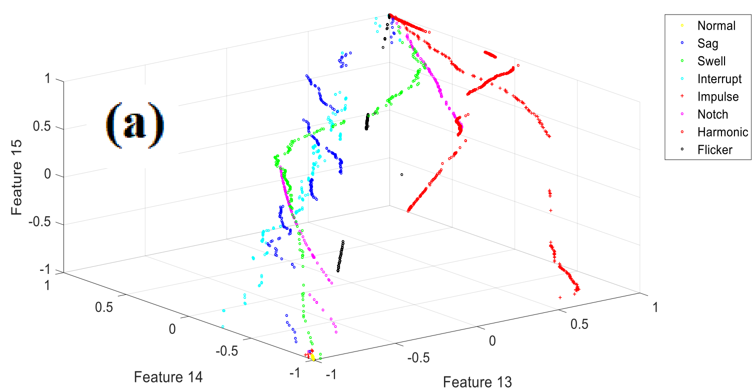

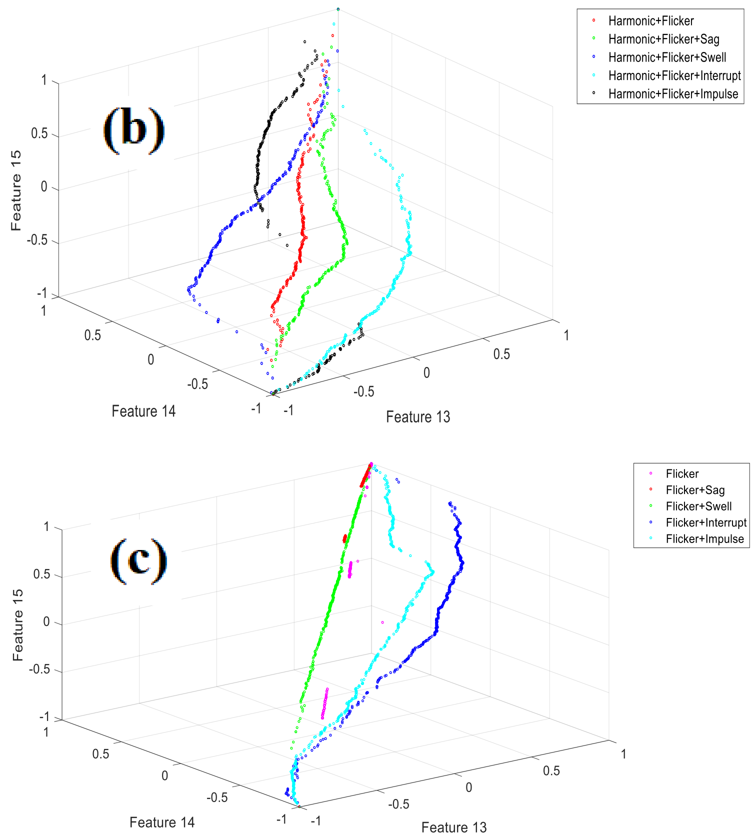

Figure 11. 3D figures of separation results: (a) individual PQDs; (b) double combination of harmonic disturbances; (c) triple combination of PQDs

5. CONCLUSION

This paper presents a novel approach with high accuracy based on the VMD and KNN for identification of complex combination of PQDs in hybrid modern power systems. In this paper, the VMD method was used to decompose the voltage signals. This method is a robust method to noise and sampling. The results of different experiments on combined PQDs show that this method has better performance in extraction of PQD features than similar methods. In this paper, in addition to classifying the PQDs, identifying their sources is also performed. In this paper, in order to evaluate the proposed method in noisy conditions, three signal-to-noise ratios of 20 dB, 30 dB, and 50 dB were investigated. The obtained results confirm that the proposed method is robust to noise and has a high accuracy in identifying the combined PQDs and their sources even in noisy conditions. To classify the PQDs only waveforms of voltages were used. To verify the proposed method, different scenarios such as half-load to full-load, variation of sun radiation and wind speed, misfiring of DE, etc. were considered. Furthermore, to verify the proposed method, our method was compared with PNN and different distance functions of KNN. Also, two feature selectors Relief-F and CFS were compared together. Results show that the accuracy and speed of the Cityblock of KNN are better than other distance functions and PNN. Also, the performance of Relief-F is better than CFS in this problem. The obtained results verify that the proposed method has a high accuracy even for combined PQDs. This approach can be used as an added tool for smart metering in modern power systems and smart power systems.

6. REFERENCES

1. Yahyazadeh, M., Johari, M.S. and HosseinNia, S.H., "Novel particle swarm optimization algorithm based on president election: Applied to a renewable hybrid power system controller", ***International Journal of Engineering, Transactions A: Basics***, Vol. 34, No. 1, (2021), 97-109, doi: 10.5829/ije.2021.34.01a.12.

2. Chandra, A. and Geng, H., "Power quality in microgrids based on distributed generators, MDPI AG, (2019), doi: 10.3390/books978-3-03928-007-0.

3. Ahmadi, M., Sharafi, P., Mousavi, M.H. and Veysi, F., "Power quality improvement in microgrids using statcom under unbalanced voltage conditions", ***International Journal of Engineering, Transactions C: Aspects***, Vol. 34, No. 6, (2021), 1455-1467, doi: 10.5829/ije.2021.34.06c.09.

4. Abdolrahimi, H. and Arab Khaburi, D., "A novel model predictive voltage control of brushless cascade doubly-fed induction generator in stand-alone power generation system", ***International Journal of Engineering, Transactions B: Applications***, Vol. 34, No. 5, (2021), 1239-1249, doi: 10.5829/ije.2021.34.05b.17.

5. Heidari, H. and Tarafdar Hagh, M., "Optimal reconfiguration of solar photovoltaic arrays using a fast parallelized particle swarm optimization in confront of partial shading", ***International Journal of Engineering***, ***Transactions B: Applications,*** Vol. 32, No. 8, (2019), 1177-1185, doi: 10.5829/ije.2019.32.08b.14.

6. Mahela, O.P., Khan, B., Alhelou, H.H. and Siano, P., "Power quality assessment and event detection in distribution network with wind energy penetration using stockwell transform and fuzzy clustering", ***IEEE Transactions on Industrial Informatics***, Vol. 16, No. 11, (2020), 6922-6932, doi: 10.1109/TII.2020.2971709.

7. Prasad, E.N., Dash, P. and Sahani, M., "Diagnosing utility grid disturbances in photovoltaic integrated dc microgrid using adaptive multiscale morphology with dfa analysis", ***Sustainable Energy, Grids and Networks***, Vol. 1, No. 1, (2021), 100574, doi: 10.1016/j.segan.2021.100574.

8. Gonzalez-Abreu, A.-D., Delgado-Prieto, M., Osornio-Rios, R.-A., Saucedo-Dorantes, J.-J. and Romero-Troncoso, R.-d.-J., "A novel deep learning-based diagnosis method applied to power quality disturbances", ***Energies***, Vol. 14, No. 10, (2021), 2839, doi: 10.3390/en14102839.

9. Cortes-Robles, O., Barocio, E., Obushevs, A., Korba, P. and Sevilla, F.R.S., "Fast-training feedforward neural network for multi-scale power quality monitoring in power systems with distributed generation sources", ***Measurement***, Vol. 170, No.1, (2021), 108690, doi: 10.1016/j.measurement.2019.107453.

10. Shen, Y., Abubakar, M., Liu, H. and Hussain, F., "Power quality disturbance monitoring and classification based on improved pca and convolution neural network for wind-grid distribution systems", ***Energies***, Vol. 12, No. 7, (2019), 1280, doi: 10.3390/en12071280.

11. Igual, R. and Medrano, C., "Research challenges in real-time classification of power quality disturbances applicable to microgrids: A systematic review", ***Renewable and Sustainable Energy Reviews***, Vol. 132, No. 1, (2020), 110050, doi: 10.1016/j.rser.2020.110050.

12. Pinto, L.S., Assunção, M.V., Ribeiro, D.A., Ferreira, D.D., Huallpa, B.N., Silva, L.R. and Duque, C.A., "Compression method of power quality disturbances based on independent component analysis and fast fourier transform", ***Electric Power Systems Research***, Vol. 187, No. 1, (2020), 106428, doi: 10.1016/j.epsr.2020.106428.

13. Ukil, A., Yeap, Y.M. and Satpathi, K., Frequency-domain based fault detection: Application of short-time fourier transform, in Fault analysis and protection system design for dc grids. 2020, Springer. 195-221, doi: 10.1007/978-981-15-2977-1_6.

14. Rahmani, A. and Deihimi, A., "Reduction of harmonic monitors and estimation of voltage harmonics in distribution networks using wavelet analysis and NARX", ***Electric Power Systems Research***, Vol. 178, No. 1, (2020), 106046, doi: 10.1016/j.epsr.2019.106046.

15. Erişti, H., Uçar, A. and Demir, Y., "Wavelet-based feature extraction and selection for classification of power system disturbances using support vector machines", ***Electric Power Systems Research***, Vol. 80, No. 7, (2010), 743-752, doi: 10.1016/j.epsr.2009.09.021.

16. Khokhar, S., Zin, A.M., Mokhtar, A., Bhayo, M. and Naderipour, A., "Automatic classification of single and hybrid power quality disturbances using wavelet transform and modular probabilistic neural network", in 2015 IEEE Conference on Energy Conversion (CENCON), IEEE. Vol. 1, No. 1, (2015), 457-462, doi: 10.1109/CENCON.2015.7409588.

17. Qiu, W., Tang, Q., Liu, J., Teng, Z. and Yao, W., "Power quality disturbances recognition using modified s transform and parallel stack sparse auto-encoder", ***Electric Power Systems Research***, Vol. 174, No. 1, (2019), 105876, doi: 10.1016/j.epsr.2019.105876

18. Senroy, N., Suryanarayanan, S. and Ribeiro, P.F., "An improved hilbert–huang method for analysis of time-varying waveforms in power quality", ***IEEE Transactions on Power Systems***, Vol. 22, No. 4, (2007), 1843-1850, doi: 10.1109/TPWRS.2007.907542.

19. Rodriguez, M.A., Sotomonte, J.F., Cifuentes, J. and Bueno-López, M., "A classification method for power-quality disturbances using hilbert–huang transform and lstm recurrent neural networks", ***Journal of Electrical Engineering & Technology***, Vol. 16, No. 1, (2021), 249-266, doi: 10.1007/s42835-020-00612-5.

20. Eristi, B., Yildirim, O., Eristi, H. and Demir, Y., "A new embedded power quality event classification system based on the wavelet transform", ***International Transactions on Electrical Energy Systems***, Vol. 28, No. 9, (2018), e2597, doi: 10.1002/etep.2597.

21. Huang, N., Peng, H., Cai, G. and Chen, J., "Power quality disturbances feature selection and recognition using optimal multi-resolution fast s-transform and cart algorithm", ***Energies***, Vol. 9, No. 11, (2016), 927, doi: 10.3390/en9110927.

22. Gholami, M., "Islanding detection method of distributed generation based on wavenet", ***International Journal of Engineering***, ***Transactions B: Applications,*** Vol. 32, No. 2, (2019), 242-248, doi: 10.5829/ije.2019.32.02b.09.

23. Wang, J. and Cheng, Z., "Wind speed interval prediction model based on variational mode decomposition and multi-objective optimization", ***Applied Soft Computing***, Vol. 113, No. 1, (2021), 107848, doi: doi.org/10.1016/j.asoc.2021.107848.

24. Pankaj, D., Govind, D. and Narayanankutty, K., "A novel method for removing rician noise from mri based on variational mode decomposition", ***Biomedical Signal Processing and Control***, Vol. 69, No. 1, (2021), 102737, doi: 10.1016/j.bspc.2021.102737.

25. Jalilian, A. and Samadinasab, S., "Detection of short-term voltage disturbances and harmonics using μpmu-based variational mode extraction method", ***IEEE Transactions on Instrumentation and Measurement***, Vol. 70, No. 1, (2021), 1-17, doi: 10.1109/TIM.2021.3075744.

26. Samanta, I.S., Rout, P.K. and Mishra, S., "An optimal extreme learning-based classification method for power quality events using fractional fourier transform", ***Neural Computing and Applications***, Vol. 33, No. 10, (2021), 4979-4995, doi: 10.1007/s00521-020-05282-y.

27. Motlagh, S.Z. and Foroud, A.A., "Power quality disturbances recognition using adaptive chirp mode pursuit and grasshopper optimized support vector machines", ***Measurement***, Vol. 168, No. 1, (2021), 108461, doi: 10.1016/j.measurement.2020.108461.

28. Sanjeevikumar, P., Sharmeela, C., Holm-Nielsen, J.B. and Sivaraman, P., "Power quality in modern power systems, Elsevier Science, (2020), doi: 10.1016/C2019-0-05409-X.

29. Sankaran, C., "Power quality, CRC Press, (2017).

30. Kharrazi, A., Sreeram, V. and Mishra, Y., "Assessment techniques of the impact of grid-tied rooftop photovoltaic generation on the power quality of low voltage distribution network-a review", ***Renewable and Sustainable Energy Reviews***, Vol. 120, No. 1, (2020), doi: 109643, 10.1016/j.rser.2019.109643

31. Saini, M.K. and Beniwal, R.K., "Detection and classification of power quality disturbances in wind-grid integrated system using fast time-time transform and small residual-extreme learning machine", ***International Transactions on Electrical Energy Systems***, Vol. 28, No. 4, (2018), e2519, doi: 10.1002/etep.2519.

32. Kazeminejad, M., Banejad, M., Annakkage, U.D. and Hosseinzadeh, N., "Load pattern-based voltage stability analysis

in unbalanced distribution networks considering maximum penetration level of distributed generation", ***IET Renewable Power Generation***, Vol. 14, No. 13, (2020), 2517-2525, doi: 10.1049/iet-rpg.2019.1196.

33. Fooladi, M., Foroud, A.A. and Abdoos, A.A., "Detection and evaluation of effective factors on flicker phenomenon in diesel-engine driven generators", ***Applied Thermal Engineering***, Vol. 113, No. 1, (2017), 1194-1207, doi: 10.1016/j.applthermaleng.2016.11.113.
34. Doustmohammadi, H. and Akbari Foroud, A., "A novel flicker detection method for vertical axis wind turbine using two-dimensional discrete wavelet transform", ***International Transactions on Electrical Energy Systems***, Vol. 30, No. 11, (2020), e12584, doi: 10.1002/2050-7038.12584.
35. Dragomiretskiy, K. and Zosso, D., "Variational mode decomposition", ***IEEE Transactions on Signal Processing***, Vol. 62, No. 3, (2013), 531-544, doi: 10.1109/TSP.2013.2288675.
36. Ali, M., Prasad, R., Xiang, Y., Khan, M., Farooque, A.A., Zong, T. and Yaseen, Z.M., "Variational mode decomposition based random forest model for solar radiation forecasting: New emerging machine learning technology", ***Energy Reports***, Vol. 7, No. 1, (2021), 6700-6717, doi: 10.1016/j.egyr.2021.09.113.
37. Hafiz, F., Swain, A., Naik, C. and Patel, N., "Feature selection for power quality event identification", in TENCON 2017-2017 IEEE Region 10 Conference, IEEE. Vol. 1, No. 1, (2017), 2984-2989, doi: 10.1109/TENCON.2017.8228373.
38. Kumar, V., Chhabra, J.K. and Kumar, D., Impact of distance measures on the performance of clustering algorithms, in Intelligent computing, networking, and informatics. 2014, Springer.183-190, doi: 10.1007/978-81-322-1665-0_17.
39. Akbari Foroud, A. and Hajian, M., "Discrimination of power quality distorted signals based on time-frequency analysis and probabilistic neural network", ***International Journal of Engineering***, ***Transactions C: Aspects,*** Vol. 27, No. 6, (2014), 881-888, doi:10.5829/idosi.ije.2014.27.06c.06.
40. Bhadane, K.V., Ballal, M.S., Nayyar, A., Patil, D.P., Jaware, T.H. and Shukla, H.P., "A comprehensive study of harmonic pollution in large penetrated grid-connected wind farm", ***MAPAN***, Vol. 1, No. 1, (2020), 1, doi: 10.1007/s12647-020-00407-z.
41. Choudhary, B., "An advanced genetic algorithm with improved support vector machine for multi-class classification of real power quality events", ***Electric Power Systems Research***, Vol. 191, No. 1, (2021), 106879, doi: 10.1016/j.epsr.2020.106879.
42. Enshaee, A. and Enshaee, P., "A new s-transform-based method for identification of power quality disturbances", ***Arabian Journal for Science and Engineering***, Vol. 43, No. 6, (2018), 2817-2832, doi: 10.1007/s13369-017-2895-2.
43. Hajian, M. and Foroud, A.A., "A new hybrid pattern recognition scheme for automatic discrimination of power quality disturbances", ***Measurement***, Vol. 51, No. 1, (2014), 265-280, doi:10.1016/j.measurement.2014.02.017.
44. Khokhar, S., Zin, A.A.M., Memon, A.P. and Mokhtar, A.S., "A new optimal feature selection algorithm for classification of power quality disturbances using discrete wavelet transform and probabilistic neural network", ***Measurement***, Vol. 95, (2017), 246-259, doi: 10.1016/j.measurement.2016.10.013.
45. Sahani, M., Dash, P. and Samal, D., "A real-time power quality events recognition using variational mode decomposition and online-sequential extreme learning machine", ***Measurement***, Vol. 157, No. 1, (2020), 107597, doi: 10.1016/j.measurement.2020.107597
46. Satish, R., Vaisakh, K., Abdelaziz, A.Y. and El-Shahat, A., "A novel three-phase power flow algorithm for the evaluation of the impact of renewable energy sources and d-statcom devices on unbalanced radial distribution networks", ***Energies***, Vol. 14, No. 19, (2021), 6152, doi: 10.3390/en14196152.
47. Cortes-Robles, O., Barocio, E., Segundo, J., Guillen, D. and Olivares-Galvan, J., "A qualitative-quantitative hybrid approach for power quality disturbance monitoring on microgrid systems", ***Measurement***, Vol.1 154, No. 1, (2020), 107453, doi: 10.1016/j.measurement.2019.107453

Persian Abstract

چکیده

شناسایی وقایع ترکیبی کیفیت توان در سیستم های قدرت مدرن با در نظر گرفتن توسعه انواع مختلف بارها و تولیدات پراکنده، اهمیت روزافزونی یافته است. نوآوری این مقاله از شناسایی دقیق و سریع وقایع ترکیبی کیفیت توان در حضور انواع مختلف بارها و تولیدات پراکنده مانند سلول فتوولتائیک، توربین بادی با ژنراتور القایی دو سو تغذیه شونده، موتور دیزلی، کوره قوس الکتریکی، ماشین‌های DC، بارهای دارای یکسوساز ٦ پالسه و ١٢ پالسه منشأ می‌گیرد. در این مقاله، ویژگی ها با استفاده از تجزیه حالت متغیر، فقط از شکل موج های ولتاژ استخراج می شوند. روش Relief-F و روش انتخاب ویژگی همبستگی به منظور کاهش داده‌های اضافی، کاهش ابعاد بردار ویژگی‌ها و زمان، بر روی ویژگی‌های استخراج‌شده اعمال شده و این دو روش با هم مقایسه می‌شوند. در این مقاله، طبقه‌بندی‌کننده k نزدیک‌ترین همسایه‌ها برای طبقه‌بندی وقایع چندگانه کیفیت توان استفاده می‌شود. به منظور بررسی اثربخشی روش پیشنهادی، سناریوهای مختلفی مانند احتراق ناقص، تغییر تابش خورشید و تغییر سرعت باد، ورود و خروج بارها، خازن‌ها و تولیدات پراکنده و خطاهای مختلف در شبکه از میان باری تا بار کامل شبیه‌سازی شده‌اند. این روش می تواند به عنوان یک الگوریتم برای دستگاه‌های اندازه‌گیری هوشمند در سیستم های برق مدرن و هوشمند مورد استفاده قرار گیرد.